Int J Appl Earth Obs Geoinformation 66 (2018) 174–183

Contents lists available at ScienceDirect

Int J Appl Earth Obs Geoinformation

journal homepage: www.elsevier.com/locate/jag

Updating stand-level forest inventories using airborne laser scanning and Landsat time series data

Douglas K. Bolton[a,*], Joanne C. White[b], Michael A. Wulder[b], Nicholas C. Coops[a], Txomin Hermosilla[a], Xiaoping Yuan[c]

[a] Integrated Remote Sensing Studio, Department of Forest Resources Management, Faculty of Forestry, University of British Columbia, 2424 Main Mall, Vancouver, British Columbia, V6T 1Z4, Canada
[b] Canadian Forest Service (Pacific Forestry Centre), Natural Resources Canada, 506 West Burnside Road, Victoria, British Columbia, V8Z 1M5, Canada
[c] Forest Analysis and Inventory Branch,Forest Stewardship Division, Ministry of Forests, Lands, Natural Resource Operations and Rural Development, PO Box 9512, Station Provincial Government, Victoria, BC, V8W 9C2, Canada

ARTICLE INFO

Keywords:
Remote sensing
Multispectral imagery
Forest attributes
Imputation
Time series
Lidar

ABSTRACT

Vertical forest structure can be mapped over large areas by combining samples of airborne laser scanning (ALS) data with wall-to-wall spatial data, such as Landsat imagery. Here, we use samples of ALS data and Landsat time-series metrics to produce estimates of top height, basal area, and net stem volume for two timber supply areas near Kamloops, British Columbia, Canada, using an imputation approach. Both single-year and time series metrics were calculated from annual, gap-free Landsat reflectance composites representing 1984–2014. Metrics included long-term means of vegetation indices, as well as measures of the variance and slope of the indices through time. Terrain metrics, generated from a 30 m digital elevation model, were also included as predictors. We found that imputation models improved with the inclusion of Landsat time series metrics when compared to single-year Landsat metrics (relative RMSE decreased from 22.8% to 16.5% for top height, from 32.1% to 23.3% for basal area, and from 45.6% to 34.1% for net stem volume). Landsat metrics that characterized 30-years of stand history resulted in more accurate models (for all three structural attributes) than Landsat metrics that characterized only the most recent 10 or 20 years of stand history. To test model transferability, we compared imputed attributes against ALS-based estimates in nearby forest blocks (> 150,000 ha) that were not included in model training or testing. Landsat-imputed attributes correlated strongly to ALS-based estimates in these blocks (R^2 = 0.62 and relative RMSE = 13.1% for top height, R^2 = 0.75 and relative RMSE = 17.8% for basal area, and R^2 = 0.67 and relative RMSE = 26.5% for net stem volume), indicating model transferability. These findings suggest that in areas containing spatially-limited ALS data acquisitions, imputation models, and Landsat time series and terrain metrics can be effectively used to produce wall-to-wall estimates of key inventory attributes, providing an opportunity to update estimates of forest attributes in areas where inventory information is either out of date or non-existent.

1. Introduction

Forest inventories are generated to support a variety of information needs ranging from operational to strategic. Data required to support these information needs likewise vary in terms of spatial and temporal resolution. In Canada, extensive forest management practices (Wulder et al., 2007) have led to the dominance of strategic-level forest inventories generated from air photo interpretation and ground sampling (Leckie and Gillis, 1995). However, these inventories are preferentially generated for managed forest areas, which represent only 65% of Canada's total forest area (Bernier et al., 2012). The remaining unmanaged forest areas have no systematic inventory information. Moreover, many of the existing forest inventories in the managed forest area are more than 20 years old, creating a need for up-to-date, cost-effective, strategic forest information to support applications such as projections of timber supply.

Airborne laser scanning (ALS) is an active remote sensing technology that enables three-dimensional forest structure to be characterized over larger spatial scales than is possible with conventional field methods (Lim et al., 2003). The use of ALS data has transformed forest inventory practices in many jurisdictions (White et al., 2016), and when combined with high quality ground plot data—in what is

* Corresponding author.
E-mail address: douglas.bolton@ubc.ca (D.K. Bolton).

https://doi.org/10.1016/j.jag.2017.11.016
Received 17 September 2017; Received in revised form 29 November 2017; Accepted 30 November 2017
Available online 08 December 2017

commonly referred to as an area-based approach (Næsset, 2002)—can produce attribute estimates that typically meet or exceed inventory accuracy requirements (Magnussen et al., 2012). Acquisitions of ALS data in Canada to support forest inventories have been increasing steadily over the past decade (D'Eon and Macafee, 2016), although the acquisitions have not been systematic and often target specific management areas of interest. Despite the pace of change in many regions, there is a need to generate and/or update strategic-level forest inventory information more rapidly over large areas, particularly in jurisdictions that have experienced widespread disturbance, such as via wildfire or as caused by the mountain pine beetle in British Columbia.

To address information needs in forests that lack ALS or inventory data, or where these data are out-of-date, optical remote sensing data can be used to estimate forest attributes from nearby ALS data collections to generate up-to-date and spatially extensive estimates of forest attributes (Frazier et al., 2014; Pflugmacher et al., 2014, 2012; Zald et al., 2016). Specifically, the sensors onboard the Landsat series of satellites have been collecting multispectral data of the planet continuously from 1982 to the present at 30-m spatial resolution, and back to 1972 at 60-m resolution, although prior to 1984, the acquisition of 30 m data was sparse (Goward et al., 2006). Following the opening of the Landsat archive in 2008 (Wulder et al., 2012a), along with advances in computing (hardware and software; Wulder and Coops, 2014), cloud masking (Zhu and Woodcock, 2014) and surface reflectance generation (Masek et al., 2006), approaches have been developed that utilize all available Landsat imagery to characterize forest change (Zhu, 2017). This Landsat time series information has been used in past research to extrapolate ALS-derived estimates of forest attributes (Frazier et al., 2014; Pflugmacher et al., 2012; Zald et al., 2016), with Pflugmacher et al. (2012) demonstrating that the inclusion of Landsat time series data improves model results over models that rely on a single date of Landsat imagery alone.

K-Nearest Neighbor (kNN) imputation has been widely used to produce wall-to-wall estimates of forest attributes using remotely sensed data (Andersen et al., 2011; Beaudoin et al., 2014; Bright et al., 2014; Hudak et al., 2008; Makela and Pekkarinen, 2004; Mora et al., 2013), given that the technique is non-parametric and can support multi-variate analysis (Chirici et al., 2016). In most applications, forest attributes are imputed directly from field plots or inventory data to spatially extensive remote sensing layers (e.g., Makela and Pekkarinen, 2004; Tomppo et al., 2008; Beaudoin et al., 2014). In Alaskan boreal forests, however, Andersen et al. (2011) found that incorporating ALS data in a two-stage approach led to improved estimates of biomass across the landscape when compared to imputing directly from field plots. Specifically, estimates of forest attributes were first derived along ALS transects by developing models between ground plots and ALS metrics. Second, these ALS-derived forest attributes were used as input data to impute forest attributes across the area of interest using Landsat imagery and synthetic aperture radar (SAR) data. Given the large area covered by the ALS transects, a wider range of structural variability could be supplied to the imputation models, leading to increased estimation accuracy. Similarly, Wilkes et al. (2015) implemented a two-stage approach that used ALS data in combination with a range of satellite data products to estimate canopy height across 2.9 million ha of forest in Victoria, Australia with a relative Root Mean Square Error (RMSE) of < 31% when compared to independent field plots. In addition to incorporating optical imagery from Landsat and the Moderate Resolution Imaging Spectroradiometer (MODIS), Wilkes et al. (2015) also included climate data, topographic information, and soil maps as predictors to produce wall-to-wall maps of canopy height.

In order to implement a two-stage approach to estimating forest attributes, highly accurate estimates of forest attributes from ALS data are first required. The area-based approach has become a standard and accepted method for generating high accuracy estimates of forest attributes over large areas with ALS data (Næsset, 2014; Wulder et al., 2013). First, discrete point clouds of ALS data are summarized using a suite of metrics that describe vegetation cover, stand height, and the vertical distribution of ALS returns (Bouvier et al., 2015; Lefsky et al., 2005; Tompalski et al., 2015). Second, through parametric (Næsset et al., 2004; Woods et al., 2011; Wulder et al., 2012b) or non-parametric (Hudak et al., 2008; Penner et al., 2013) approaches, these ALS metrics are related against field measured forest attributes, such stem volume or basal area. Finally, the developed models are then applied to predict forest attributes wall-to-wall across the ALS data collection.

Given the incrementally developing coverage of ALS data that exist across many jurisdictions, an opportunity exists to explore how these high-quality datasets can be leveraged to provide wall-to-wall estimates of key forest attributes in areas where ALS data have not been collected and where existing inventory data is out of date. In this analysis, we develop a methodology to produce models that impute forest attributes using a suite of Landsat single-year and time series predictors near Kamloops, British Columbia, Canada, where ALS data was collected and forest attributes were predicted in 2014 for several spatially disjointed areas covering approximately 350,000 ha. Through this analysis, we ask the following specific questions.

1.1. How does the predictive capability of imputation models for top height, basal area, and stem volume change when single-year Landsat metrics are replaced with Landsat time series metrics?

Most attempts to predict forest attributes with Landsat time series information have relied on metrics that describe disturbance and recovery dynamics (e.g., Pflugmacher et al., 2012; Frazier et al., 2014). However, as many sampled stands within our study area have not undergone a major disturbance during the interval of the Landsat recorded we assessed (1984–2014), information on disturbance and recovery from 1984 to 2014 is not likely informative for many stands. Alternatively, time series metrics such as long-term spectral means, variability of spectral indices through time, and the slope of indices through time, can describe long-term stand conditions and development, regardless of disturbance history. Here, we assess the relative importance of Landsat predictor variables that describe single-year spectral conditions and disturbance history versus metrics that describe long-term spectral conditions, with a special interest on undisturbed stands.

1.2. For LANDSAT time series predictors, what length of time yields the best results for making attribute estimates: 10-year, 20-year, or 30-year descriptors?

Landsat time series metrics can be calculated across a number of time periods. Longer periods of time will capture more of a stand's history (e.g., 30 year spectral averages), while shorter time periods will more accurately describe the current state of a forest stand (e.g., 10 year spectral averages). To determine how the length of time described impacts model accuracy, we compare Landsat time-series metrics calculated at 10, 20, and 30 years prior to the year of the ALS data collection (2014).

1.3. How well do pixel-level imputation models estimate forest structure at the stand-level?

Landscape-level decision making for forest management is not often made for individual grid cells (pixels) from remotely sensed data products, but rather for stand-level polygons. In British Columbia, stand-level polygons are derived for managed forests through the Vegetation Resources Inventory (VRI), which is a forest inventory program developed by British Columbia's Ministry of Forests, Lands Natural Resource Operations (MFLNRO). Stand-level boundaries are derived in the VRI through photo interpretation, and are combined with a sample of ground plots to produce inventory data across British Columbia (Sandvoss et al., 2005). To determine if imputed forest attributes can accurately capture variability at the scale at which management decisions are made, we compare imputed estimates against ALS estimates at

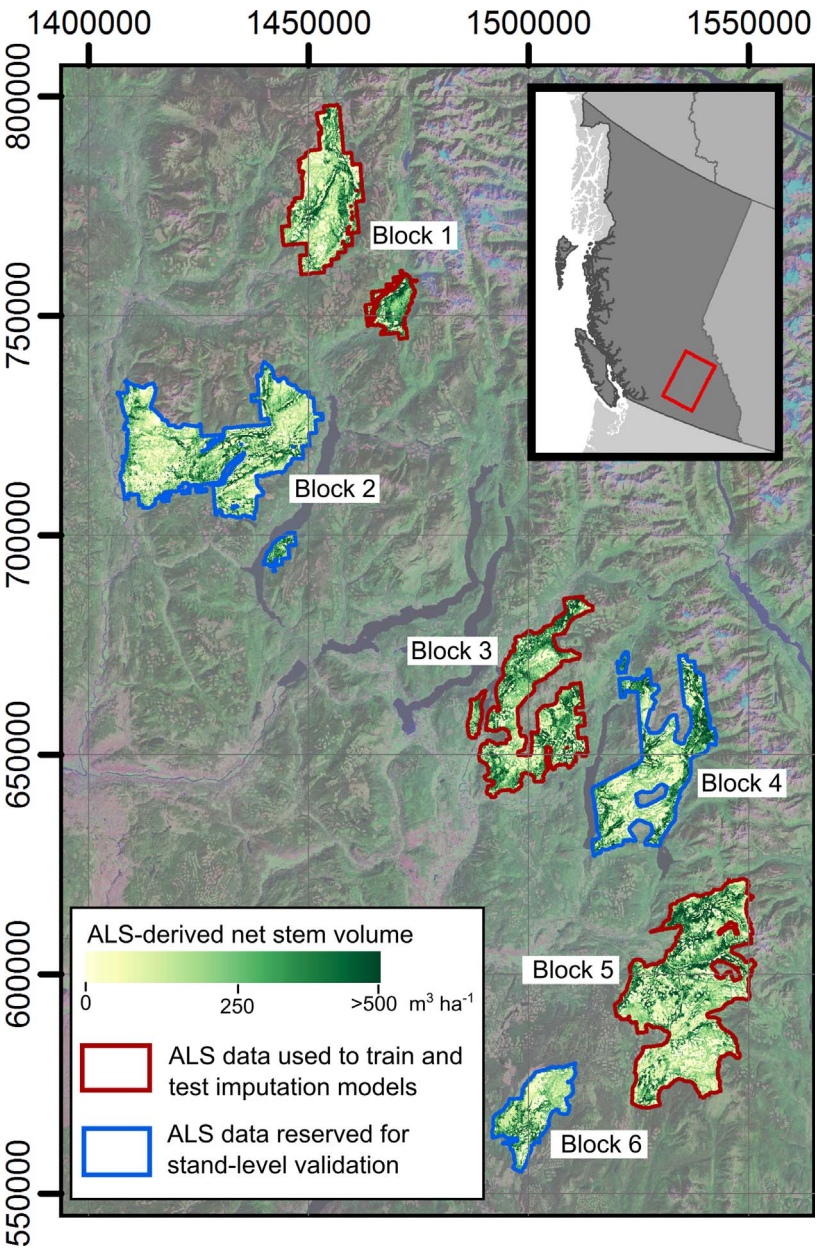

Fig. 1. ALS coverage near Kamloops, British Columbia, Canada. Blocks in red were used to train and test the imputation models. Blocks in blue were used to perform a stand-level comparison between ALS-derived attributes and Landsat imputed estimates. (For interpretation of the references to colour in this figure legend, the reader is referred to the web version of this article.)

the VRI stand-level. As the goal is to determine how well imputation models describe variability in forest structure outside of areas where ALS data has already been acquired, the stand-level comparison will be made in forested areas not included in model training and testing, allowing model transferability to be assessed.

2. Methods

2.1. Study area

This study was conducted across two timber supply areas near Kamloops, British Columbia, representing a total area of approximately 350,000 ha (Fig. 1). According to the ecosystem classification in British Columbia, the area of interest is dominated by two Biogeoclimatic Ecosystem Classification (BEC) zones: Engelmann Spruce-Subalpine Fir (ESSF) and Interior Cedar–Hemlock (ICH), with area proportions of 41% and 49%, respectively. Two minor BEC zones are also present: Montane Spruce (MS, 3%) and Interior Douglas fir (IDF, 8%). The ESSF occurs in relatively cold, moist, and snowy continental climate mountainous terrain that is often steep and rugged (elevation 1200–2100 m). Engelmann spruce (*Picea engelmannii*) and subalpine fir (*Abies lasiocarpa*) are the dominant tree species in the ESSF. Spruce usually dominates the canopy of mature stands. Subalpine fir is most abundant in the understory, however, at high elevations and in some wetter areas, it frequently dominates the forest canopy. The ICH occurs at lower to middle elevations (400–1500 m) with the highest diversity of tree species of any zone in the province. Western redcedar (*Thuja plicata*) and Western hemlock (*Tsuga heterophylla*) are the two dominant tree species. Other dominant species such as Douglas fir (*Pseudotsuga menziesii*) and lodgepole pine (*Pinus contorta*) are present in MS and IDF. The Montane Spruce is a transitional zone between ESSF and IDF with mixed tree species such as spruce, subalpine fir, Douglas fir and lodgepole pine.

2.2. Data sources

2.2.1. ALS-derived estimates of forest attributes

ALS-derived estimates of forest attributes were obtained from the

Ministry of Forests, Lands, Natural Resource Operations (MFLNRO) for areas near Kamloops, British Columbia (Fig. 1). The estimates of forest attributes cover 350,000 ha and were generated using an area-based approach at a 20-m spatial resolution from ALS data collected in 2014. MFLNRO derived these estimates of forest attributes by building area-based models between 233 circular ground plots (fixed radius of 11.28 m) and a standard suite of ALS metrics that describe the vertical distribution and density of ALS returns within each plot (please see White et al., 2013 for more information on conducting an area-based inventory with ALS data). Here, we focus on ALS-derived estimates of basal area, top height, and net stem volume as these attributes are of particular interest to forest managers. Basal area was measured for all live trees with a diameter at breast height (DBH) > 4 cm, while net stem volume was defined as the net merchantable stem volume for all live trees with a DBH > 12.5 cm. Top height was determined by measuring the height of the largest diameter live tree in dominant and co-dominant layers within 5.64 m of plot center, regardless of species or residual status. These estimates from ALS data were derived for six distinct forest blocks (see Fig. 1). In this study, three blocks were used for model training and testing, while the remaining three blocks were reserved for an independent comparison between imputed values and ALS estimates at the VRI stand-level. Summary statistics for each block are presented in Table 1

2.2.2. Landsat time-series data

Landsat time-series predictors and forest disturbance information were derived from gap-filled Landsat composites for 1984–2016 produced following the Composite 2 Change (C2C) approach (Hermosilla et al., 2017, 2016). Specifically, best-available pixel (BAP) image composites were first produced from Landsat imagery by selecting observations for each pixel within a specific date range (August 1 +/ −30 days) based on the scoring functions defined by White et al. (2014), which rank the presence and distance to clouds and their shadows, the atmospheric quality, and the acquisition sensor. Next, these image composites were further refined by removing noisy observations (e.g., haze and smoke) and infilling data gaps using spectral trend analysis of pixel time series (Hermosilla et al., 2015a). Implementation of these rules and subsequent temporal analysis allows for the production of seamless annual surface reflectance composites for all of Canada, as well as the detection and characterization of forest change events. Hermosilla et al. (2016) reported the overall national detection accuracy for change events (1984–2012) was 89.0%. Following the object-based image analysis approach introduced in Hermosilla et al. (2015b), the detected changes were attributed to a change type (i.e., fire, harvesting, road, or non-stand-replacing such as insect disturbance), based on their spectral, temporal, and geometrical characteristics using a Random Forests classifier, with an overall accuracy of 92% (please see Hermosilla et al., 2016 for an overview of the generation of image composites and change products).

Tasseled Cap Brightness (TCB), Greenness (TCG), Wetness (TCW), and Tasseled Cap Angle (TCA) were calculated for each annual gap-free composite from 1984 to 2014 (Crist, 1985; Pflugmacher et al., 2012).

Table 1
Mean and standard deviations for ALS-derived estimates of top height, basal area, and net stem volume for the six blocks displayed in Fig. 1. Standard deviations are in parentheses.

Forest Attribute	Block 1	Block 2	Block 3	Block 4	Block 5	Blockb6
Top height [m]	34.1 (18.2)	30.5 (15.9)	37.8 (17.3)	34.9 (18.9)	31.9 (18.1)	30.2 (14.3)
Basal area [m^2/ha]	22.4 (7.1)	21.3 (7.3)	24.7 (7.0)	23.9 (7.9)	22.4 (8.3)	21.8 (7.8)
Net stem volume [m^3/ha]	235.3 (147.1)	205.4 (133.5)	274.1 (151.0)	254.9 (167.6)	229.4 (159.5)	210.7 (125.1)

TCA was calculated as TCA = atan(TCG/TCB). Two variables were included to describe disturbance: c hange type and years since disturbance. Disturbances were classified as either stand replacing (fire, harvest, or road) or non-stand replacing. If a pixel was not disturbed between 1984 and 2014, years since disturbance was set to 50 years. Availing upon the BAP image composites and associated attributed change information produced by C2C, a land cover data set has also been produced. This land cover dataset was used to create a forest/non-forest mask to constrain the analysis described herein.

2.2.3. Topographic data

Topographic information for the study area was obtained from the Canadian Digital Elevation Model (CDEM). The CDEM is produced by Natural Resources Canada at scales of 1:50,000 and 1:250,000, derived primarily from data from the National Topographic Data Base (NTDB). The 1:50,000 product, which is delivered at a spatial resolution of 0.75 ″ (~ 23 m), was obtained for this analysis and resampled to derive a 30 m spatial resolution digital elevation model for the study area (Natural Resources Canada, 2017). From the digital elevation model, slope and the topographic solar radiation index (TSRI) were also calculated. TSRI is a transformed measure of aspect, obtained as TSRI = 0.5 − cos((π/180)(aspect − 30))/2. TSRI can take values between 0, indicating cold NE slopes, and 1, indicating warm SW slopes. Topographic variables were resampled to 30 m to align with the Landsat predictor variables.

2.2.4. Vegetation resources inventory data

To assess how Landsat imputed attributes compare to lidar-derived estimates at the stand-level, Vegetation Resources Inventory (VRI) polygons from 2013 were obtained (British Columbia Data Catalogue, 2017a). The polygons were derived through visual interpretation of aerial photos, with each polygon representing a delineated forest stand (relating a unit of homogeneity with regards to forest age, composition, and structure). VRI represents the standard of forest inventory data in British Columbia, and is used by both land managers and the provincial government to inform decision making on the landscape. Across the study area, VRI polygons averaged 14 ha in size, with a maximum polygon size of 806 ha. Historical information on the date of harvest for VRI polygons was also obtained (British Columbia Data Catalogue, 2017b), which will be used as a tool to interpret model predictions. While differences in forest inventories exist by jurisdiction, both within (Leckie and Gillis, 1995) and between (Kangas and Maltamo, 2006) countries, the notion of linking a suite of descriptive attributes to a spatial unit is common. As such, the update approach presented here is applicable outside of the current implementation jurisdiction.

2.3. Building imputation models

To integrate ALS-derived forest attributes (20 m spatial resolution) with Landsat variables (30 m spatial resolution), ALS cells were assigned a 5 × 5 cell average of each forest attribute, representing a surrounding area of 100 m by 100 m, while Landsat and topographic variables were assigned 3 × 3 cell averages, representing an area of 90 m by 90 m. The ALS-derived attributes were then resampled to the Landsat grid using a nearest neighbour approach to produce both sets of attributes on a 30 m grid. While the 30 m cells represented a 90 by 90 m average for Landsat spectral data, the value of the center 30 m cell was retained for Landsat disturbance variables that could not be averaged (change type and years since change). In Alaskan boreal forests, Strunk et al. (2014) found an improved relationship between ground plots, lidar, and Landsat data for estimating forest attributes at 90 × 90 m compared to 30 × 30 m (Strunk et al., 2014). Spatial error in either the Landsat or lidar data could lead to mismatches between spectral metrics and structural variables, contributing to errors in estimation. In addition, the minimum stand size for strategic forest inventories in British Columbia is 2 ha; therefore these attribute estimates at the 90 m cells

are sufficient for augmenting forest inventories across the province. In general, it is understood that larger plots (from lidar) are more robust to alterations in positon (geolocation) and for representing local conditions as edge-effects are minimized (Frazer et al., 2011).

To focus the analysis on forested areas only, non-forested areas were masked using the 2012 land cover classification (as described above). As 2012 was the most recent year that land cover information was available, an additional step was required to remove forests that were harvested between 2012 and 2014, as these areas would no longer be considered forested at the time of the ALS flight. Specifically, areas that were classified as a stand replacing disturbance (i.e, harvest, fire, or road) between 2012 and 2014 in the C2C approach were masked from the analysis. Once forested areas were isolated, random samples were selected for model training and testing. To ensure that the models could predict across the full range of structural conditions present in the study area, the forested area was first stratified into 20 classes based on the ALS-derived estimates of forest attributes. Specifically, a k-means clustering procedure was performed using the estimates of top height, basal area, and net stem volume. A stratified random sample of training cells was then selected, with the number of training cells in each of the 20 classes proportional to the presence of those classes across the landscape. As nearby cells are often spatially autocorrelated and do not represent independent samples for model development, randomly sampled cells were required to be at least 500 m apart. Additionally, to avoid selecting training cells on forest edges, all adjacent 30 m pixels were required to be forested (i.e., 3 × 3 cell window). In total, three-thousand 30 m pixels were randomly distributed across blocks one, three, and five, representing 0.18% of the forested area in these blocks. This set of random pixels was divided into a training (75%, 2250 samples) and testing (25%, 750 samples) set.

Once training cells were selected, predictor variables were calculated for each cell. These variables included single-year Landsat predictors derived from the 2014 BAP composite, time series predictors derived from gap-filled Landsat composites from 1984 to 2014, information on disturbance history from 1984 to 2014, and topographic variables. To test the predictive capabilities of single-year Landsat metrics versus Landsat time series metrics, as well as the predictive capability of Landsat time-series metrics at different temporal lengths, six model scenarios were run. A summary of these model scenarios and their associated set of predictors is summarized in Table 2. Each model scenario was run to predict top height, basal area, and net stem volume using k-NN imputation, with the random forests proximity matrix used to derive the nearest neighbour distance metric (Liaw and Wiener, 2002). Specifically, the yai function of the yaImpute package was used for the imputation (Crookston and Finley, 2008), with the number of regression trees set to 500 and the number of nearest neighbors set to one. Once each model was trained on the 2250 training samples, the models were applied to the remaining 750 testing samples, and the accuracy of each model was assessed using the coefficient of determination (R^2) between observed and predicted values, the root mean squared error (RMSE), and the model bias. RMSE and bias were calculated as follows:

$$\text{RMSE} = \sqrt{\frac{1}{n}\sum_{i=1}^{n}(Predicted_i - Observed_i)^2} \quad (1)$$

$$\text{Bias} = \frac{1}{n}\sum_{i=1}^{n}(Predicted_i - Observed_i) \quad (2)$$

where $Observed_i$ is the ALS-derived estimate for the ith test sample and $Predicted_i$ is the imputed value for each model. Relative RMSE and bias (RMSE%, bias%) were calculated relative to the mean of the observed values.

2.4. Comparing estimates at the VRI stand-level

Once a candidate model for top height, basal area, and net stem volume was selected, imputed values were produced for blocks two, four, and six (see Fig. 1) and compared against ALS-derived estimates at the VRI stand-level. Each VRI polygon was assigned the average values for both the imputed attributes and the ALS-derived attributes. Only forested cells were considered when calculating the averages (i.e., classified as forest in 2012, no stand replacing disturbance between 2012 and 2014). Only VRI polygons that were > 2 ha in size and > 75% forested according to the 2012 land cover classification were assessed (6645 polygons in total). As blocks two, four, and six were not included in model training and testing, this additional comparison will allow us to assess the transferability of imputation models to nearby areas without ALS data, and provide an understanding of how well the models perform at the stand-level.

Table 2
Predictor variables for each model scenario. All model scenarios include topographic variables. Filled boxes represent the variables used in each model.

Predictor Variables	**Model A:** Single-year predictors	**Model B:** Single-year and change predictors	**Model C:** 10-year predictors	**Model D:** 20-year predictors	**Model E:** 30-year predictors	**Model F:** Single-year, change, and 30-year predictors
Single date metrics						
2014 TCB, TCG, TCW, TCA	■	■				■
Time series metrics						
Mean, standard deviation, slope of TCB, TCG, TCW, TCA (2005 - 2014)			■			
Mean, standard deviation, slope of TCB, TCG, TCW, TCA (1995 - 2014)				■		
Mean, standard deviation, slope of TCB, TCG, TCW, TCA (1985 - 2014)					■	■
Landsat change metrics						
Change type, Years since change		■				■
Topographic metrics						
Elevation, Slope, TSRI	■	■	■	■	■	■

Table 3
R^2 values between observed and predicted attributes for 750 held-out samples. See Table 1 for a list of predictor variables for each model.

Forest Attribute	Model A: Single-year predictors	Model B: Single-year and change predictors	Model C: 10-year predictors	Model D: 20-year predictors	Model E: 30-year predictors	Model F: Single-year, change, and 30-year predictors
Top height	0.25	0.38	0.38	0.51	0.54	0.55
Basal area	0.42	0.52	0.52	0.63	0.66	0.65
Net stem volume	0.33	0.41	0.41	0.53	0.57	0.55

Table 4
Relative RMSEs and relative bias between observed and predicted attributes for 750 held-out samples. Bias is displayed in parentheses. See Table 2 for a list of predictor variables for each model.

Forest Attribute	Model A: Single-year predictors	Model B: Single-year and change predictors	Model C: 10-year predictors	Model D: 20-year predictors	Model E: 30-year predictors	Model F:Single-year, change, and 30-year predictors
Top height	22.8% (0.2%)	20.1% (−0.3%)	19.8% (−1.1%)	17.1% (−0.8%)	16.5% (−1.2%)	16.4% (−1.1%)
Basal area	32.1% (−0.6%)	28.7% (−0.7%)	28.9% (−2.3%)	24.5% (−1%)	23.3% (−1.2%)	23.7% (−1.2%)
Net stem volume	45.6% (−0.5%)	41.7% (−0.7%)	41.9% (−3%)	35.7% (−1.6%)	34.1% (−2.1%)	34.9% (−1.9%)

3. Results

Table 3 displays the coefficient of determination (R^2) values between observed and predicted estimates of top height, basal area, and net volume for 750 test samples in each model scenario, while Table 4 displays the relative Root Mean Square Error (RMSE) and bias for each model. Of the three predicted attributes, basal area consistently had the strongest level of agreement between observed and predicted values (R^2 = 0.42–0.66), followed by whole stem volume (R^2 = 0.33–0.57), and top height (R^2 = 0.25–0.55). Alternatively, top height had the lowest relative RMSE (RMSE% = 16.5–22.8%), followed by basal area (RMSE% = 23.3–32.1%), and whole stem volume (RMSE% = 34.1–45.6%).

The R^2 values were lowest (R^2 = 0.25–0.42) and RMSEs highest (RMSE = 22.8%–45.6%) for model A, which included single-year Landsat predictors and topographic information. Model performance improved when Landsat change metrics (i.e., years since change and change type) were added in model B (R^2 = 0.38–0.52). Model performance did not improve when single-year predictors were replaced with 10-year Landsat predictors in model C (R^2 = 0.38–0.52, RMSE = 19.8%–41.9%); however, as the length of the temporal metrics increased from 10-years to 30-years, R^2 values increased and RMSE values decreased (R^2 = 0.54–0.66, RMSE = 16.5%–34.1% for model E). Model accuracy did not improve when single-year and change metrics were added in model F (R^2 = 0.55–0.65, RMSE = 16.4%–34.9%), therefore model E was chosen as the candidate model. Scatterplots between observed and predicted values for model E are displayed in Fig. 2. Fig. 3 displays the scaled variable importance for model E. Elevation was the most important variable in the model, followed by the 30-year mean TCW, TCG slope, TCB slope, TCA mean, and the standard deviation of TCW. TSRI was the least important variable in the model.

3.1. Comparing estimates at the VRI stand level

Fig. 4 displays the stand-level comparisons between ALS estimates and model E predictions for forest blocks not included in model development (i.e., blocks two, four, and six in Fig. 1). Agreement between model estimates was strongest for basal area (R^2 = 0.75), followed by net stem volume (R^2 = 0.67) and top height (R^2 = 0.62). Alternatively, the relative RMSE was lowest for top height (RMSE = 13.1%), followed by basal area (RMSE = 17.8%), and net stem volume (RMSE = 26.5%). All three attributes had a negative bias (i.e., imputed values were consistently lower than ALS estimates), with the largest bias for net stem volume (−7.8%), followed by basal area (−6.1%), and top height (−3.7%).

Fig. 5 displays ALS-derived estimates of net stem volume, as well as volume estimates imputed using model B and E, for block six (southeast corner of study area). When compared against the ALS-derived estimates, model B and E both captured the general patterns of volume across the block, with high volume estimates in the southwest corner, trending to low volume estimates in the northwest corner. However, key differences in volume predictions were observed in areas that were harvested between 1970 and 1983 (i.e., prior to the start of the Landsat

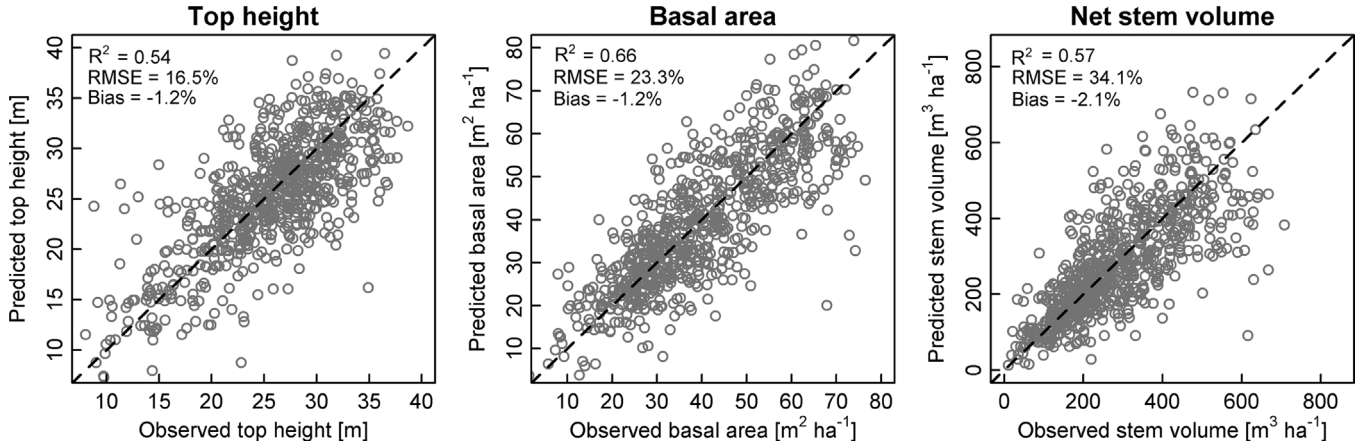

Fig. 2. Scatterplots between observed and predicted attributes for 750 held-out samples using 30-year Landsat predictors (Model E). Observed values are ALS-derived estimates of forest attributes.

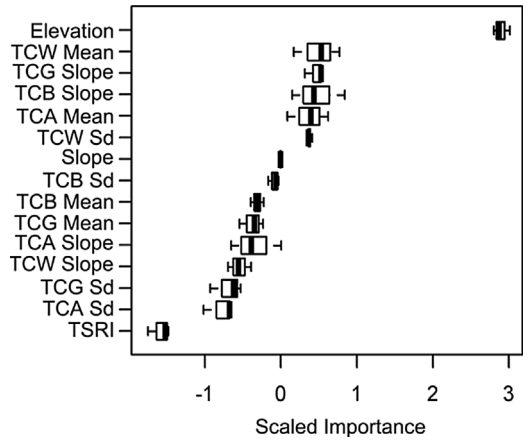

Fig. 3. Scaled importance values for Model E (30-year Landsat metrics and topographic predictors). Scaled importance values were derived using the yaiVarImp function in the yaImpute package in R (Crookston and Finley, 2008). Scaled values were obtained by calculating z-scores from the importance values.

time-series). Specifically, model E was better able than model B to capture the spatial patterns in volume associated with these harvested areas, while model B tended to predict higher volumes than ALS over these harvested areas.

4. Discussion

Existing ALS-derived estimates of forest attributes can be leveraged in combination with Landsat time series and terrain metrics to estimate key forest attributes where inventory data does not exist, or where inventories are out-of-date. Previous research (e.g., Pflugmacher et al., 2012) has demonstrated that Landsat time series is more capable of explaining variability in forest attributes than single-year Landsat predictors alone. The model accuracy reported herein confirm the findings of Pflugmacher et al. (2012) when using Landsat time series predictors (Pflugmacher et al. reported a relative RMSE of 28% for basal area, 41% for aboveground biomass, and 30% for Lorey's height). However, while previous studies have focused mainly on Landsat predictors that relate to disturbance and recovery dynamics (Main-Knorn et al., 2013; Pflugmacher et al., 2012; Zald et al., 2016), we have demonstrated that simple long-term spectral averages and measures of temporal variability have strong predictive power. Moreover, we found that the inclusion of disturbance information alone did not greatly improve model accuracy (model A to model B), as most of the sampled stands in our study area had not undergone a major disturbance in the past 30 years. This finding demonstrates the need for additional time series metrics that do not explicitly describe disturbance.

Landsat time series variables were particularly important in areas that were disturbed immediately prior to the start of our Landsat time series (pre-1984). Specifically, model B overestimated volume in areas that were harvested between 1970 and 1983 (Fig. 5), as the canopies in these cutblocks likely closed by 2014 (i.e., corresponding to the year of the single-year Landsat predictors). Optical satellite measurements are less sensitive to variability in forest structure once canopies close (Avitabile et al., 2012, 2011; Duncanson et al., 2010; Wulder et al., 1996). Therefore, models that only incorporate single-year Landsat metrics after canopy closure will not be as sensitive to structural differences between stands. Model B did incorporate Landsat change metrics (year of change, type of change) in addition to single-year predictors, but because the disturbances occurred prior to 1984, these disturbances were not captured by these metrics. Alternatively, model E was able to capture forest structural variability in and around these cutblocks, as the 30-year predictors inform on stand condition early in the time series prior to canopy closure. This ability to describe stand history in areas that were not disturbed during the Landsat record is likely why model E outperformed model B. However, incorporating Landsat Multispectral Scanner (MSS) data could allow a longer record of discrete disturbances to be incorporated (back to 1972), which would likely improve the predictive capability of change metrics across the landscape. It is important to note that while discrete changes in forest condition (e.g., fire and harvest) are feasible to derive from Landsat MSS data, additional time series metrics may prove challenging to incorporate in imputation models given the different spectral, spatial, and radiometric resolutions of Landsat MSS data.

Increasing the length of the Landsat time series appears to improve the predictive capability of imputation models, as the accuracy increased from model C (10-year predictors) to model E (30-year predictors). The superior performance of model E suggests that it is more important to observe a stand's history, than it is to accurately characterize the current state of the forest (via single-year metrics). However, 30-year metrics may not be appropriate for all applications, as models using 30-year metrics are unable to make historical predictions of forest structure. Specifically, model E could only be used to make attribute predictions for 2013–2016, as 30 previous years of Landsat data are required. Alternatively, if single-year predictors are used, models could be applied to predict forest attributes annually from 1984 to 2016, but at a lower accuracy (assuming similar results to those presented herein). Knowledge of a terminal structural status (from lidar) can also be used to guide estimation of prior conditions (such as in Pflugmacher et al., 2012; Ahmed et al., 2014). While accurate estimates of current structure are critical to land managers, historical

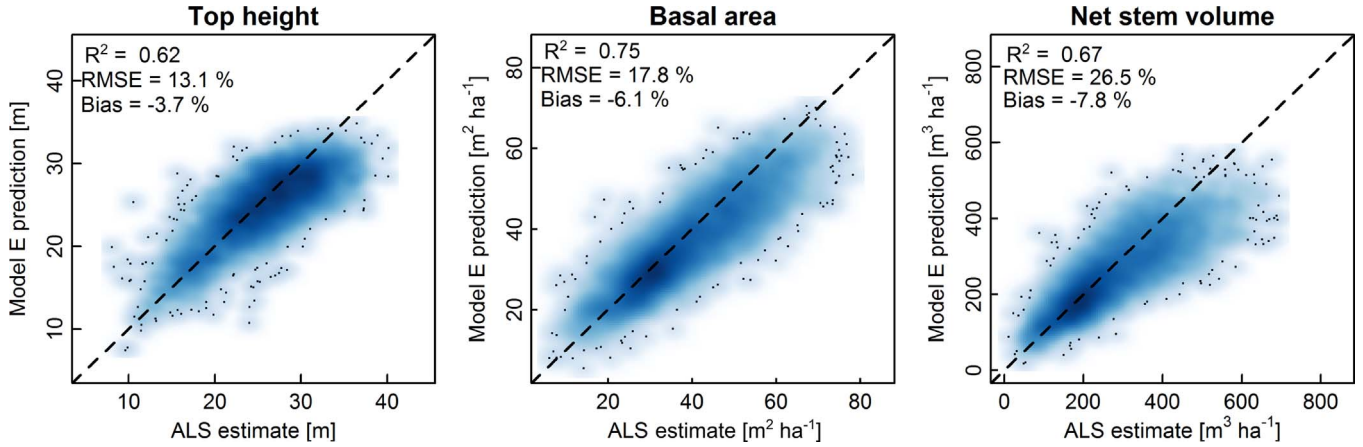

Fig. 4. Stand-level comparisons between ALS estimates and best performing imputation model (Model E) predictions (30-year predictors). Stands represent inventory polygons, delineated via air photo interpretation and derived from British Columbia's Vegetation Resources Inventory (VRI) program. Only areas in blocks two, four, and six from Fig. 1 are included, as these areas were excluded from model training and testing (6645 VRI polygons in total).

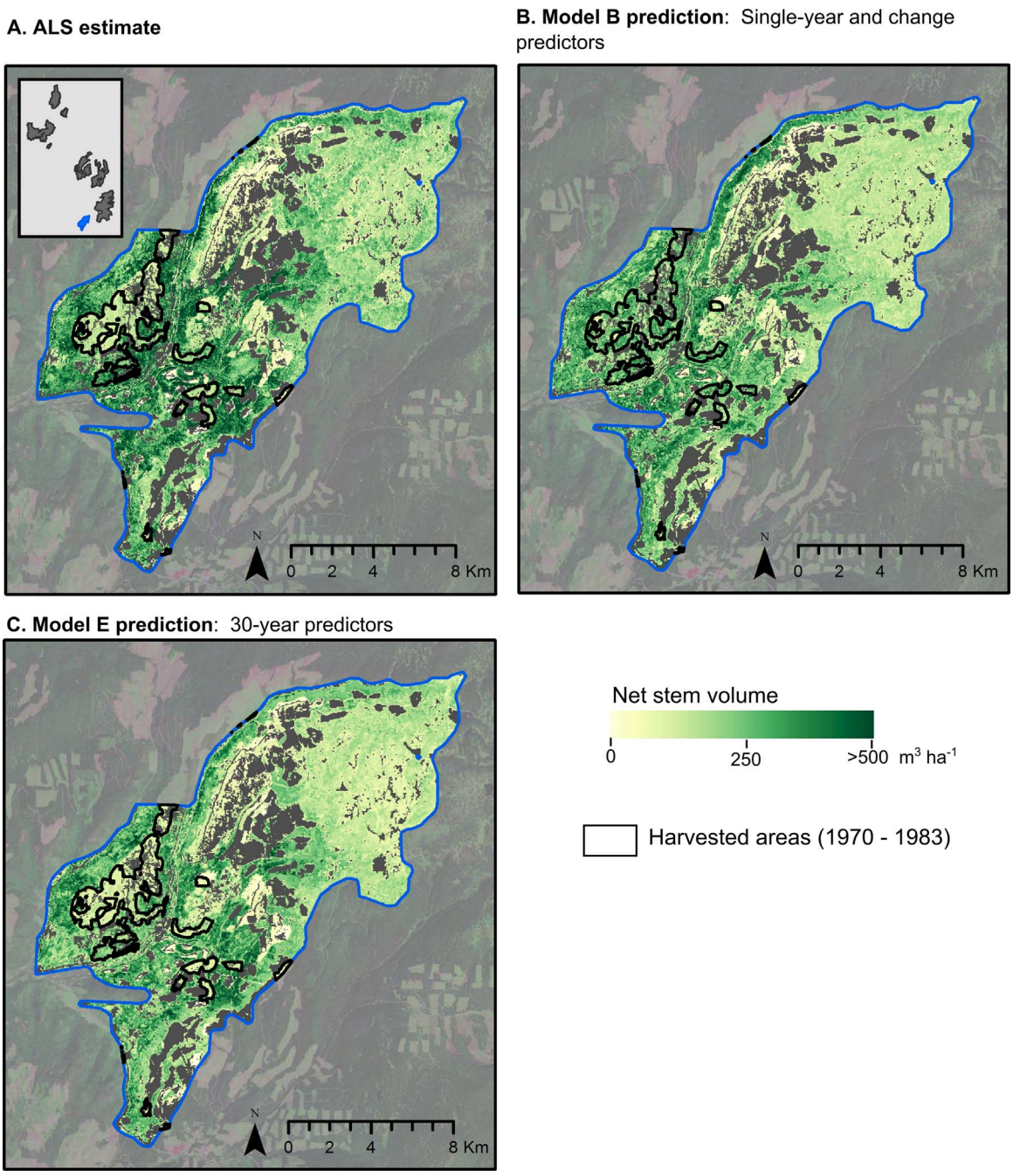

Fig. 5. A) ALS estimates of net stem volume for block six (southeast corner of study area); B) Net stem volume predictions using Model B; C) Net stem volume predictions using Model E. Areas harvested between 1970 and 1983 are outlined to demonstrate the differences between Model B and Model E for areas harvested prior to the start of the Landsat time-series (pre-1984).

information on structure is important for monitoring changes in habitats, monitoring carbon budgets, as well as tracking growth. Therefore, determining the balance between model accuracy and the ability to make historical estimates will vary depending on specific applications and information needs.

Limitations of Landsat vegetation indices in closed canopies may have contributed to the slight underestimations of forest attributes observed in mature, productive stands (i.e., tall stands with high basal area and high volume), leading to negative model biases (−1.2–−2.1% for Model E). Specifically, as Landsat vegetation indices are less sensitive to structural variability once canopies close (Avitabile et al., 2012, 2011; Duncanson et al., 2010; Wulder et al., 1996), estimation error will likely be highest in stands that had dense, closed canopies for the entire time series (1984–2014). This is observable in Fig. 2c, as stem volumes > 500 m^3/ha tended to be under predicted. However, as biases remained small, this issue was not a major concern.

Imputation models were able to accurately predict forest attributes at the VRI stand-level for forest blocks not included in model training and testing (RMSE = 13.1–26.5%), demonstrating the transferability of the models, and the ability to make estimates at the scale of interest to land managers. However, model bias was slightly higher when the models were transferred to the new blocks (Bias = −3.9–−8.0%), suggesting that the full range of structural variability in the new blocks may not have been captured in the training plots used in model development. In order to generate wall-to-wall estimates across large study areas, it is critical that the full range of structural variability is

captured by the training samples to avoid underestimations in productive stands, or overestimations in unproductive stands. If similar imputation models are applied wall-to-wall across British Columbia, capturing the full range of structural variability with existing ALS datasets alone may prove difficult, as most ALS data collections are focused in the province's more productive, managed forest areas. Therefore, government and university led initiatives to collect ALS data in unmanaged forests, such as the ~25,000 km of transects of ALS data collected across boreal Canada in 2010 (Wulder et al., 2012b), are critical to ensure that low productivity forests are represented in imputation models.

Elevation was the most important variable in the models, highlighting the importance of including ancillary variables in the imputation process. Elevation was particularly important given the large elevational gradient over the study area, which resulted in a gradient in forest type, from highly productive Interior Cedar − Hemlock forests at lower elevations to Engelmann Spruce-Subalpine Fir forests at high elevations. Mean TCW was the most important spectral variable in the model, but similar importance values were observed for the TCB slope, TCG slope, TCA mean, and TCW standard deviation, suggesting that both average measurements and measures of variability are important in imputation models. Wilkes et al. (2015) and Zald et al. (2016) also found TCW to be the most important spectral variable in imputation models to predict forest attributes, demonstrating the value of spectral indices that rely on the mid-infrared portion of the spectrum, where Landsat bands are sensitive to moisture content (Cohen, 1991; Cohen and Goward, 2004).

While we have demonstrated that Landsat imputation models can produce estimates of forest attributes that are comparable to stand-level estimates derived from ALS data, the true accuracy of these models will largely depend on the quality of the area-based ALS-derived estimates used to train the models. ALS data has been used extensively to derive highly accurate estimates of key forest attributes, but in order for forest managers to achieve high accuracies, a series of best practices must be followed, which includes establishing a sample of ground plots that capture the full range of forest structural variability observed in the ALS data, as well as minimizing the time lag between ALS data collection and field measurements (White et al., 2013). Provided standard practices for the area-based approach are followed, then estimates of forest attributes derived from ALS data will remain a valuable source of input data for estimating forest attributes wall-to-wall over large study areas through the use of imputation models.

Historically, the generation of forest inventory information via air photo interpretation provided a cost-effective means of data collection over very large areas (Leckie and Gillis, 1995). The use of skilled human interpreters somewhat mitigated the lack of spatial or categorical detail available from the photos, as a function of the experience and expertise of the interpreters. At the time, these strategic-level inventories provided the best-available information for applications such as timber supply projection; however, the subjectivity of photointerpretation and associated errors in forest inventories have been documented in the literature, with Thompson et al. (2007) reporting an error rate of 30–60% for interpreted estimates of species composition. Currently, as the number of skilled photo interpreters declines, and as the transition to digital acquisition and attribution processes continues, many trade-offs in the production of inventory information are emerging. For instance, ALS data provides for greater accuracy, precision, and spatial detail, but the relatively higher costs (compared to photos) have resulted in smaller acquisition areas. As a result, forest management agencies may have to focus their limited resources on priority areas, leading to a subset of high quality ALS-based forest inventory information on a portion of the management area, with increasingly dated and generalized data elsewhere. Opportunities, such as presented herein, to use ALS data collected over a limited portion of the management area to aid in the broader characterization of a given jurisdiction are required. Our results demonstrate that forest management agencies have alternative options for producing and maintaining strategic-level forest inventory information.

5. Conclusions

Spatially-limited ALS acquisitions, in combination with Landsat time-series data and terrain metrics, can be effectively used to derive temporally and spatially consistent strategic-level estimates of top height, basal area, and net stem volume in areas that lack such information or where existing forest inventories are out-of-date. Landsat metrics that described long-term spectral averages and spectral variability were better able to estimate top height, basal area, and net stem volume than models using single-year Landsat metrics. While digital data and approaches are becoming increasingly adopted, photo-based forest inventories remain common for capture and portrayal of strategic-level forest inventory information, and could thus be considered as the quality benchmark against which new and emerging technologies are compared. ALS-derived estimates of forest attributes offer information at an operational level of detail, beyond that of large area strategic inventory activities. Use of the ALS-derived attributes as the comparative standard in this research indicates that the update capacity and attribute information quality afforded by the Landsat-based imputation approach presented herein are sufficient for strategic inventory purposes.

Acknowledgements

This research was supported by the Canadian Wood Fibre Centre (CWFC) of the Canadian Forest Service, Natural Resources Canada. Support was also provided by a Natural Sciences and Engineering Research Council of Canada (NSERC) grant to Nicholas Coops. In addition, we thank Christopher Butson and Ann Morrison of MFLNRO for additional support in working with the ALS-derived forest attribute layers.

References

Ahmed, O.S., Franklin, S.E., Wulder, M.A., 2014. Interpretation of forest disturbance using a time series of Landsat imagery and canopy structure from airborne lidar. Can. J. Remote Sens. 39, 521–542. http://dx.doi.org/10.5589/m14-004.

Andersen, H.E., Strunk, J., Temesgen, H., Atwood, D., Winterberger, K., 2011. Using multilevel remote sensing and ground data to estimate forest biomass resources in remote regions: a case study in the boreal forests of interior Alaska. Can. J. Remote Sens. 37, 596–611. http://dx.doi.org/10.5589/m12-003.

Avitabile, V., Herold, M., Henry, M., Schmullius, C., 2011. Mapping biomass with remote sensing: a comparison of methods for the case study of Uganda. Carbon Balance Manage. 6. http://dx.doi.org/10.1186/1750-0680-6-7.

Avitabile, V., Baccini, A., Friedl, M.A., Schmullius, C., 2012. Capabilities and limitations of Landsat and land cover data for aboveground woody biomass estimation of Uganda. Remote Sens. Environ. 117, 366–380. http://dx.doi.org/10.1016/j.rse.2011.10.012.

Beaudoin, A., Bernier, P.Y., Guindon, L., Villemaire, P., Guo, X.J., Stinson, G., Bergeron, T., Magnussen, S., Hall, R.J., 2014. Mapping attributes of Canada's forests at moderate resolution through k NN and MODIS imagery. Can. J. For. Res. 44, 521–532. http://dx.doi.org/10.1139/cjfr-2013-0401.

Bernier, P., Kurz, W.A., Lempriere, T., Ste-Marie, C., 2012. A Blueprint for Forest Carbon Science in Canada 2012–2020. Natural Resources Canada, Ottawa, ON.

Bouvier, M., Durrieu, S., Fournier, R. a., Renaud, J.-P., 2015. Generalizing predictive models of forest inventory attributes using an area-based approach with airborne LiDAR data. Remote Sens. Environ. 156, 322–334. http://dx.doi.org/10.1016/j.rse.2014.10.004.

Bright, B.C., Hudak, A.T., Kennedy, R.E., Meddens, A.J.H., 2014. Landsat time series and lidar as predictors of live and dead basal area across five bark beetle-Affected forests. IEEE J. Sel. Top. Appl. Earth Obs. Remote Sens. 7, 3440–3452. http://dx.doi.org/10.1109/JSTARS.2014.2346955.

British Columbia Data Catalogue, 2017a. VRI - Forest Vegetation Composite Polygons and Rank 1 Layer. https://catalogue.data.gov.bc.ca/dataset/vri-forest-vegetation-composite-polygons-and-rank-1-layer.

British Columbia Data Catalogue, 2017b. Harvested Areas of BC. https://catalogue.data.gov.bc.ca/dataset/harvested-areas-of-bc-consolidated-cutblocks.

Chirici, G., Mura, M., McInerney, D., Py, N., Tomppo, E.O., Waser, L.T., Travaglini, D., McRoberts, R.E., 2016. A meta-analysis and review of the literature on the k-Nearest Neighbors technique for forestry applications that use remotely sensed data. Remote Sens. Environ. 176, 282–294. http://dx.doi.org/10.1016/j.rse.2016.02.001.

Cohen, W.B., Goward, S.N., 2004. Landsat's role in ecological applications of remote sensing. Bioscience 54, 535–545.
Cohen, W.B., 1991. Response of vegetation indices to changes in three measures of leaf water stress. Photogramm. Eng. Remote Sens. 57, 195–202.
Crist, E.P., 1985. A TM tasseled cap equivalent transformation for reflectance factor data. Remote Sens. Environ. 17, 301–306.
Crookston, N.L., Finley, A.O., 2008. yaImpute: an R package for kNN imputation. J. Stat. Softw. 23, 1–16.
D'Eon, S.D., Macafee, K., 2016. Knowledge exchange in the Canadian Wood Fibre Centre: national scope with regional delivery. For. Chronical 92, 441–446.
Duncanson, L.I., Niemann, K.O., Wulder, M.A., 2010. Integration of GLAS and Landsat TM data for aboveground biomass estimation. Can. J. Remote Sens. 36, 129–141. http://dx.doi.org/10.5589/m10-037.
Frazer, G.W., Magnussen, S., Wulder, M.A., Niemann, K.O., 2011. Simulated impact of sample plot size and co-registration error on the accuracy and uncertainty of LiDAR-derived estimates of forest stand biomass. Remote Sens. Environ. 115, 636–649. http://dx.doi.org/10.1016/j.rse.2010.10.008.
Frazier, R.J., Coops, N.C., Wulder, M.A., Kennedy, R., 2014. Characterization of aboveground biomass in an unmanaged boreal forest using Landsat temporal segmentation metrics. ISPRS J. Photogramm. Remote Sens. 92, 137–146. http://dx.doi.org/10.1016/j.isprsjprs.2014.03.003.
Goward, S.N., Arvidson, T.J., Williams, D.L., Faundeen, J., Irons, J., Franks, S., 2006. Historical record of Landsat global coverage: mission operations, NSLRSDA, and international cooperator stations. Photogramm. Eng. Remote Sens. 72, 710–720.
Hermosilla, T., Wulder, M., White, J.C., Coops, N., Hobart, G.W., 2015a. An integrated Landsat time series protocol for change detection and generation of annual gap-free surface reflectance composites. Remote Sens. Environ. 158, 220–234. http://dx.doi.org/10.1016/j.rse.2014.11.005.
Hermosilla, T., Wulder, M.A., White, J.C., Coops, N.C., Hobart, G.W., 2015b. Regional detection, characterization, and attribution of annual forest change from 1984 to 2012 using Landsat-derived time-series metrics. Remote Sens. Environ. 170, 121–132. http://dx.doi.org/10.1016/j.rse.2015.09.004.
Hermosilla, T., Wulder, M.A., White, J.C., Coops, N.C., Hobart, G.W., Campbell, L.B., 2016. Mass data processing of time series Landsat imagery: pixels to data products for forest monitoring. Int. J. Digit. Earth 9, 1035–1054. http://dx.doi.org/10.1080/17538947.2016.1187673.
Hermosilla, T., Wulder, M.A., White, J.C., Coops, N.C., Hobart, G.W., 2017. Updating Landsat time series of surface-reflectance composites and forest change products with new observations. Int. J. Appl. Earth Obs. Geoinf. 63, 104–111. http://dx.doi.org/10.1016/j.jag.2017.07.013.
Hudak, A.T., Crookston, N.L., Evans, J.S., Hall, D.E., Falkowski, M.J., 2008. Nearest neighbor imputation of species-level, plot-scale forest structure attributes from LiDAR data. Remote Sens. Environ. 112, 2232–2245.
Kangas, A., Maltamo, M., 2006. Managing Forest Ecosystems: Forest Inventory – Methodology and Applications. Springer Dordrecht, The Netherlands.
Leckie, D.G., Gillis, M.D., 1995. Forest inventory in Canada with emphasis on map production. For. Chron. 71, 74–88.
Lefsky, M.A., Hudak, A.T., Cohen, W.B., Acker, S.A., 2005. Patterns of covariance between forest stand and canopy structure in the Pacific Northwest. Remote Sens. Environ. 95, 517–531. http://dx.doi.org/10.1016/j.rse.2005.01.004.
Liaw, A., Wiener, M., 2002. Classification and Regression by random forest. R News 2, 18–22.
Lim, K., Treitz, P., Wulder, M.A., St-Onge, B., Flood, M., 2003. LiDAR remote sensing of forest structure. Prog. Phys. Geogr. 27, 88–106. http://dx.doi.org/10.1191/0309133303pp360ra.
Magnussen, S., Næsset, E., Gobakken, T., Frazer, G., 2012. A fine-scale model for area-based predictions of tree-size-related attributes derived from LiDAR canopy heights. Scand. J. For. Res. 27, 312–322. http://dx.doi.org/10.1080/02827581.2011.624116.
Main-Knorn, M., Cohen, W.B., Kennedy, R.E., Grodzki, W., Pflugmacher, D., Griffiths, P., Hostert, P., 2013. Monitoring coniferous forest biomass change using a Landsat trajectory-based approach. Remote Sens. Environ. 139, 277–290. http://dx.doi.org/10.1016/j.rse.2013.08.010.
Makela, H., Pekkarinen, A., 2004. Estimation of forest stand volumes by Landsat TM imagery and stand-level field-inventory data. For. Ecol. Manage. 196, 245–255. http://dx.doi.org/10.1016/j.foreco.2004.02.049.
Masek, J.G., Vermote, E.F., Saleous, N.E., Wolfe, R., Hall, F.G., Huemmrich, K.F., Gao, F., Kutler, J., Lim, T.-K., 2006. A Landsat surface reflectance dataset for North America, 1990–2000. IEEE Geosci. Remote Sens. Lett. 3, 68–72.
Mora, B., Wulder, M.A., Hobart, G.W., White, C., Bater, C.W., Gougeon, F.A., 2013. Forest inventory stand height estimates from very high spatial resolution satellite imagery calibrated with lidar plots. Int. J. Remote Sens. 34, 37–41.
Næsset, E., Gobakken, T., Holmgren, J., Hyyppa, H., Hyyppa, J., Maltamo, M., Nilsson, M., Olsson, H., Persson, A., Soderman, U., 2004. Laser scanning of forest resources: the Nordic experience. Scand. J. For. Res. 19, 482–499. http://dx.doi.org/10.1080/02827580410019553.
Næsset, E., 2002. Predicting forest stand characteristics with airborne scanning laser using a practical two-stage procedure and field data. Remote Sens. Environ. 80, 88–99.
Næsset, E., 2014. Area-Based Inventory in Norway–From Innovation to an Operational Reality, In: Forestry Applications of Airborne Laser Scanning. Springer, Dordrecht, The Netherlands, pp. 215–240. http://dx.doi.org/10.1007/978-94-017-8663-8.
Natural Resources Canada, 2017. Canadian Digital Elevation Model. http://open.canada.ca/data/en/dataset/7f245e4d-76c2-4caa-951a-45d1d2051333.
Penner, M., Pitt, D.G., Woods, M.E., 2013. Parametric vs nonparametric LiDAR models for operational forest inventory in boreal Ontario. Can. J. Remote Sens. 39, 426–443. http://dx.doi.org/10.5589/m13-049.
Pflugmacher, D., Cohen, W.B., Kennedy, R.E., 2012. Using Landsat-derived disturbance history (1972–2010) to predict current forest structure. Remote Sens. Environ. 122, 146–165. http://dx.doi.org/10.1016/j.rse.2011.09.025.
Pflugmacher, D., Cohen, W.B., Kennedy, R.E., Yang, Z., 2014. Using Landsat-derived disturbance and recovery history and lidar to map forest biomass dynamics. Remote Sens. Environ. 151, 124–137. http://dx.doi.org/10.1016/j.rse.2013.05.033.
Sandvoss, M., McClymont, B., Farnden, C., 2005. User's Guide to the Vegetation Resources Inventory. Tolko Industries, Ltd., Williams Lake, BC, Canada.
Strunk, J.L., Temesgen, H., Andersen, H.-E., Packalen, P., 2014. Prediction of forest attributes with field plots, Landsat, and a sample of lidar strips: a case study on the Kenai Peninsula, Alaska. Photogramm. Eng. Remote Sensing 80, 143–150. http://dx.doi.org/10.14358/PERS.80.2.143.
Thompson, I.D., Maher, S.C., Rouillard, D.P., Fryxell, J.M., Baker, J.A., 2007. Accuracy of forest inventory mapping: some implications for boreal forest management. For. Ecol. Manage. 252, 208–221. http://dx.doi.org/10.1016/j.foreco.2007.06.033.
Tompalski, P., Coops, N.C., White, J.C., Wulder, M.A., 2015. Enriching ALS-derived area-based estimates of volume through tree-level downscaling. Forests 6, 2608–2630. http://dx.doi.org/10.3390/f6082608.
Tomppo, E., Olsson, H., Ståhl, G., Nilsson, M., Hagner, O., Katila, M., 2008. Combining national forest inventory field plots and remote sensing data for forest databases. Remote Sens. Environ. 112, 1982–1999. http://dx.doi.org/10.1016/j.rse.2007.03.032.
White, J.C., Wulder, M.A., Varhola, A., Vastaranta, M., Coops, N.C., Cook, B.D., Pitt, D., Woods, M., 2013. A best practices guide for generating forest inventory attributes from airborne laser scanning data using an area-based approach. For. Chron. 89, 722–723. http://dx.doi.org/10.5558/tfc2013-132.
White, J.C., Wulder, M.A., Hobart, G.W., Luther, J.E., Hermosilla, T., Griffiths, P., Coops, N.C., Hall, R.J., Hostert, P., Dyk, A., Guindon, L., 2014. Pixel-based image compositing for large-area dense time series applications and science. Can. J. Remote Sens. 40, 192–212. http://dx.doi.org/10.1080/07038992.2014.945827.
White, J.C., Coops, N.C., Wulder, M.A., Vastaranta, M., Hilker, T., Tompalski, P., 2016. Remote sensing technologies for enhancing forest inventories: a review. Can. J. Remote Sens. 42, 619–641. http://dx.doi.org/10.1080/07038992.2016.1207484.
Wilkes, P., Jones, S.D., Suarez, L., Mellor, A., Woodgate, W., Soto-Berelov, M., Haywood, A., Skidmore, A.K., 2015. Mapping forest canopy height across large areas by upscaling ALS estimates with freely available satellite data. Remote Sens. 7, 12563–12587. http://dx.doi.org/10.3390/rs70912563.
Woods, M., Pitt, D., Penner, M., Lim, K., Nesbitt, D., Etheridge, D., Treitz, P., 2011. Operational implementation of a LiDAR inventory in Boreal Ontario. For. Chron. 87, 512–528. http://dx.doi.org/10.5558/tfc2011-050.
Wulder, M.A., Coops, N.C., 2014. Make Earth observations open access. Freely available satellite imagery will improve science and environmental monitoring products. Nature 513, 30–32.
Wulder, M.A., Franklin, S.E., Lavigne, M., 1996. High spatial resolution optical image texture for improved estimation of forest stand leaf area index. Can. J. Remote Sens. 22, 441–449. http://dx.doi.org/10.1080/07038992.1996.10874668.
Wulder, M.A., Campbell, C., White, J.C.C., Flannigan, M., Campbell, I.D.D., 2007. National circumstances in the international circumboreal community. For. Chron. 83, 539–556.
Wulder, M.A., Masek, J., Cohen, W., Loveland, T., Woodcock, C., 2012a. Opening the archive: how free data has enabled the science and monitoring promise of Landsat. Remote Sens. Environ. 122, 2–10. http://dx.doi.org/10.1016/j.rse.2012.01.010.
Wulder, M.A., White, J.C., Bater, C.W., Coops, N.C., Hopkinson, C., Chen, G., 2012b. Lidar plots — a new large-area data collection option: context, concepts, and case study. Can. J. Remote Sens. 38, 600–618. http://dx.doi.org/10.5589/m12-049.
Wulder, M.A., Coops, N.C., Hudak, A.T., Morsdorf, F., Nelson, R., Newnham, G., Vastaranta, M., 2013. Status and prospects for LiDAR remote sensing of forested ecosystems. Can. J. Remote Sens. 39, 1–5.
Zald, H.S.J., Wulder, M.A., White, J.C., Hilker, T., Hermosilla, T., Hobart, G.W., Coops, N.C., 2016. Integrating Landsat pixel composites and change metrics with lidar plots to predictively map forest structure and aboveground biomass in Saskatchewan. Canada. Remote Sens. Environ. 176, 188–201. http://dx.doi.org/10.1016/j.rse.2016.01.015.
Zhu, Z., Woodcock, C.E., 2014. Automated cloud, cloud shadow, and snow detection in multitemporal Landsat data: an algorithm designed specifically for monitoring land cover change. Remote Sens. Environ. 152, 217–234. http://dx.doi.org/10.1016/j.rse.2014.06.012.
Zhu, Z., 2017. Change detection using Landsat time series: a review of frequencies, preprocessing, algorithms, and applications. ISPRS J. Photogramm. Remote Sens. 130, 370–384. http://dx.doi.org/10.1016/j.isprsjprs.2017.06.013.